www.czasopisma.pan.pl PAN POLSKA AKADEMIA NAUK www.journals.pan.pl

PAN ARCHIVES OF ACOUSTICS
Vol. **37**, No. 3, pp. 287–294 (2012)

DOI: 10.2478/v10168-012-0037-0

Theoretical Studies of Nonlinear Generation Efficiency in a Bubble Layer

Anna BARANOWSKA

Faculty of Applied Physics and Mathematics
Gdańsk University of Technology
Narutowicza 11/12, 80-233 Gdańsk, Poland; e-mail: anbar@mif.pg.gda.pl

(*received October 25, 2011; accepted June 13, 2012*)

The aim of the paper is a theoretical analysis of propagation of high-intensity acoustic waves throughout a bubble layer. A simple model in the form of a layer with uniformly distributed mono-size spherical bubbles is considered. The mathematical model of the pressure wave's propagation in a bubbly liquid layer is constructed using the linear non-dissipative wave equation and assuming that oscillations of a single bubble satisfy the Rayleigh-Plesset equation. The models of the phase sound speed, changes of resonant frequency of bubbles and damping coefficients in a bubbly liquid are compared and discussed. The relations between transmitted and reflected waves and their second harmonic amplitudes are analyzed. A numerical analysis is carried out for different environmental parameters such as layer thicknesses and values of the volume fraction as well as for different parameters of generated signals. Examples of results of the numerical modeling are presented.

Keywords: nonlinear acoustics, bubble layer, transmitted and reflected waves.

1. Introduction

The nonlinear wave generation inside layers plays a very important role in practice of production of parametric sonars, where the key problem is the efficiency of their nonlinear generation. The known mathematical models of this problem consist of a set of two differential equations. The first of them, the linear non-dissipative wave equation, describes acoustic pressure changes in the bubble layer (see, for example, Druzhinin *et al.*, 1996; Vanhille, Campos–Pozuelo, 2008). The second one is an equation, which allows to predict the bubble radius changes, or equivalently, the bubble volume variations. To complete their models, some authors use the Zabolotskaya and Soluyan approach, in which the bubble volume variation changes are applied (see e.g., Hamilton, Blackstock, 1998; Vanhille, Campos–Pozuelo, 2008). Another option in the theoretical analysis is the application of the Rayleigh–Plesset equation which allows to analyze radius changes of a bubble (see, for example Leighton, 2008). Our model of bubble oscillations is based on the Rayleigh–Plesset equation. It is worth noting that in the Vanhille and Druzhin models and similar ones, it is assumed that the differences between values of density in the bubble layer and outside of it are small. Moreover, they take into account only the viscous damping constant. The model proposed by the author of this paper (Baranowska, 2011) allows to analyze the problem in a more general form. For example, it permits to include not only the viscous damping constant but also the total damping coefficient and different values of the sound speed and density inside and outside the bubble layer. In this paper, we assume that the density differences are small and the model presented in Sec. 2 takes into consideration this fact and, as a consequence, we obtain a simplified version of the general model.

It should also be mentioned that a correct choice of physical parameters is very important in the process of theoretical investigations as they influence the accuracy and the correctness of the results. One of them is the sound speed. It is possible to find many papers on modeling and measurements of this parameter in different media (for example Hamilton, Blackstock, 1998; Perelomova, Wojda, 2010). There exist a few formulae for the prediction of the behavior of this parameter in a bubbly medium. Among others there is a model proposed by Ye and Ding (1995) where the influence of multiple scattering of waves on the sound

speed is incorporated. Another one, simpler but nevertheless very popular and commonly used, is a model proposed by Commander and Prosperetti (1989). However, it does not include higher-order bubble interactions and can be used rather when the gas volume fraction is small or the frequencies of sounding signals are far from the resonance of the bubbles.

In this paper we present the results of a numerical study of the nonlinear propagation of high intensity waves in a bubbly liquid layer. The transmitted and reflected waves as a function of the incident wave frequency in relation to the bubble's resonance frequency as well as their concentration and layer thicknesses are studied. The efficiency of the generation of second harmonic components is examined and examples of computations are presented. In our work, we have considered two cases of bubble layers. In the first one, the layers are filled with bubbles of size which assures that they are at resonance with the sounding signals. In the second case, the bubble's resonance frequency is far from the sounding signals. We used the Commander and Prosperetti model to compute the phase sound speed in the bubble layer. The values of this parameter obtained by this model for higher values of the volume fraction and resonance frequency differ from those obtained by using the Ye and Ding model. However, this fact did not influence the final results of the numerical calculations significantly.

2. Mathematical model

We assume that a liquid layer (region II) of single size spherical bubbles distributed uniformly is placed between $x = 0$ and $x = L$. Figure 1 sketches out the problem studied in this paper. The density and sound speed inside the bubble layer are ρ_L and c_L, correspondingly. These parameters outside this layer are ρ_0 and c_0, respectively. Because of small differences between the density of water at the equilibrium state and in the medium with bubbles we can put $\rho_L = \rho_0$. The media outside the layer are considered to be linear liquids. In region I the acoustic field is the sum of the incident wave p_i and reflected one p_r. In region III propagates only the transmitted wave p_t.

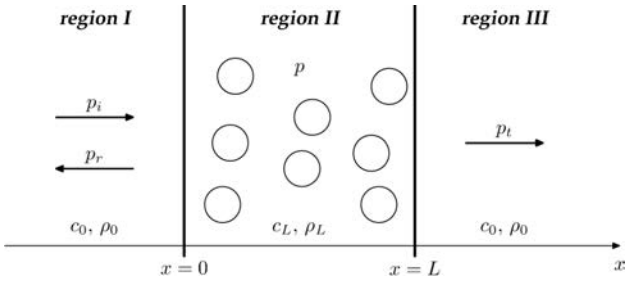

Fig. 1. Sketch of the problem.

The equation for the acoustic pressure p in the bubble layer is given in the following form (Druzhinin *et al.*, 1996; Hamilton, Blackstock, 1998; Karpov *et al.*, 2003; Baranowska, 2011):

$$\frac{\partial^2 p}{\partial x^2}(x,t) - \frac{1}{c_L^2}\frac{\partial^2 p}{\partial t^2}(x,t) = -\rho_0 \frac{\partial^2 \beta}{\partial t^2}(x,t), \tag{1}$$

where β is the local fraction of the volume occupied by the gas. Assuming a constant number N of air bubbles per unit volume, the volume fraction is given by

$$\beta(x,t) = \frac{4}{3}\pi R^3(x,t)N, \tag{2}$$

where R is the instantaneous radius of the bubbles.

The instantaneous bubble radius $R(t)$ driven by the incident signal acoustic pressure $P(t)$ is calculated using the Rayleigh–Plesset equation:

$$R\frac{\mathrm{d}^2 R}{\mathrm{d}t^2} + \frac{3}{2}\left(\frac{\mathrm{d}R}{\mathrm{d}t}\right)^2 = \frac{1}{\rho_0}\left[p_g\left(\frac{R_0}{R}\right)^{3\gamma} + p_v - p_{\mathrm{stat}} - \frac{2\sigma}{R} - P(t) - \rho_0\delta_t\omega R\frac{\mathrm{d}R}{\mathrm{d}t}\right], \tag{3}$$

where p_v is the gas and vapor pressure inside a bubble, p_{stat} is the ambient static pressure, R_0 is the equilibrium bubble radius, ω is the angular frequency, γ is the polytropic exponent of the gas, σ is the coefficient of surface tension, $p_g = 2\sigma/R_0 + p_{\mathrm{stat}} - p_v$ and δ_t is the damping coefficient for the bubble. It should be noted here that the bubble radius R and pressure P in the Rayleigh–Plesset equation (3) are only functions of the time variable t. In fact, we consider them as functions of two coordinates: the time coordinate t and the one-dimensional coordinate x putting $p(x,t)$ instead of $P(t)$.

To complete the formulation of our problem, initial and boundary conditions are defined. The initial conditions for $x \neq 0$ are as follows:

$$\begin{aligned} p(x,0) &= 0, & \frac{\partial p}{\partial t}(x,0) &= 0, \\ R(x,0) &= R_0, & \frac{\partial R}{\partial t}(x,0) &= 0. \end{aligned} \tag{4}$$

The boundary conditions are defined in the following way. The medium outside the layer is regarded as linear and non dispersive, therefore we can assume that the incident, reflected and transmitted waves have the forms

$$\begin{aligned} p_i(x,t) &= p_i(t - x/c_0), \\ p_r(x,t) &= p_r(t + x/c_0), \\ p_t(x,t) &= p_t(t - x/c_0). \end{aligned} \tag{5}$$

At the layer boundaries the pressure should be continuous, which, at $x = 0$ and $x = L$, gives

$$\begin{aligned} p(0,t) &= p_i(0,t) + p_r(0,t), \\ p(L,t) &= p_t(L,t). \end{aligned} \tag{6}$$

Taking into account the continuity of velocity or, equivalently, the pressure gradient, for $x = 0$, we have

$$\frac{\partial p_i}{\partial x}(0,t) + \frac{\partial p_r}{\partial x}(0,t) = \frac{\partial p}{\partial x}(0,t). \tag{7}$$

Taking the time derivative of (6), using (7) and the relation $\partial p_r/\partial t = c_0 \partial p_r/\partial x$ together with the analogous relation for the incident wave p_i, we eliminate the reflected wave. Finally the boundary condition for $x = 0$ is

$$\frac{\partial p}{\partial t}(0,t) - c_0 \frac{\partial p}{\partial x}(0,t) = 2\frac{\partial p_i}{\partial t}(0,t). \tag{8}$$

A similar consideration at $x = L$ leads to

$$\frac{\partial p}{\partial t}(L,t) + c_0 \frac{\partial p}{\partial x}(L,t) = 0. \tag{9}$$

Assuming a harmonic incident signal, we define for $x = 0$

$$p_i(0,t) = P_A \sin(\omega t). \tag{10}$$

We are looking for the solution of the system of Eqs. (1), (3) with initial and boundary conditions (4), (8), (9) for $x \in [0, L]$ and $t \in [0, T_{\max}]$. The finite-difference method was employed to solve equation (1), while Eq. (3) was solved using the classical fourth order Runge–Kutta method. As the result of numerical calculations we obtain the acoustic pressure $p_{i,n} = p(x_i, t_n)$ and the bubble radius $R_{i,n} = R(x_i, t_n)$ at the nodal points $x_i = i\Delta x$, $t_n = n\Delta t$, where $\Delta x = L/N_x$, $\Delta t = T_{\max}/N_t$, $i = 0, 1, \ldots, N_x$ and $n = 0, 1, \ldots, N_t$. After the calculation of $p_{i,m}$ and $R_{i,m}$ for $m \le n$, we can compute $R_{i,n+1}$ and the pressure $p_{i,n+1}$, i.e. we can compute the bubble radius and the pressure at time $t = t_{n+1}$ if we know the values of these functions for $t \le t_n$.

3. Phase sound speed, resonant frequency and damping coefficient

The phase speed of acoustic waves c_L is calculated on the basis of the dispersion relation including the effective complex wave number κ in a gas-liquid mixture. To describe the procedure of calculation, first we write the square of the complex wave number using the Ye and Ding formula (Ye, Ding, 1995):

$$\kappa^2 = k^2 + 4\pi A\left(1 - i\frac{2\pi B}{k}\right), \tag{11}$$

where

$$A = \int_0^\infty \frac{n(a)a\,\mathrm{d}a}{\omega_0^2/\omega^2 - 1 + i\delta_t}, \qquad B = \int_0^\infty \frac{n(a)a^2\,\mathrm{d}a}{(\omega_0^2/\omega^2 - 1 + i\delta_t)^2} \tag{12}$$

and $k = \omega/c_0$ is the acoustic wave number, ω_0 is the resonance angular frequency of a bubble, $n(a)$ is the number of bubbles per unit volume with radii a in the $da = 1$ μm range.

Now, we set

$$\frac{\kappa}{k} = u - iv, \tag{13}$$

where the quantities u and v are obtained using Eq. (11). Finally, the phase speed c_L is given by

$$c_L = \frac{c_o}{u}. \tag{14}$$

If the higher order term $2\pi B/k$ in Eq. (11) is ignored, we obtain the Commander and Prosperetti formula (Commander, Prosperetti, 1989):

$$\kappa^2 = k^2 + 4\pi \int_0^\infty \frac{n(a)a\,\mathrm{d}a}{\omega_0^2/\omega^2 - 1 + i\delta_t}. \tag{15}$$

In this paper we consider a bubble population with the same equilibrium radius R_0, i.e. $n(a) = N\delta(a - R_o)$ where δ denotes the Dirac delta function. After some calculations we obtain:

$$\kappa^2 = k^2 + \frac{3\beta_0/R_0^2}{\omega_0^2/\omega^2 - 1 + i\delta_t}, \tag{16}$$

where the gas volume fraction at equilibrium is given by

$$\beta_0 = \frac{4}{3}\pi R_0^3 N. \tag{17}$$

The phase sound speed depends on the bubble size distribution, the frequency of the sounding signal, the bubble resonance frequency and the bubble damping coefficient. The resonance angular frequency ω_0 of a bubble with radius R_0 can be determined using the formula (Commander, Prosperetti, 1989):

$$\omega_0^2 = \frac{p_0}{\rho_0 R_0^2}\left(\mathrm{Re}\,\Phi - \frac{2\sigma}{p_0 R_0}\right), \tag{18}$$

with

$$\Phi = \frac{3\gamma}{1 - 3(\gamma - 1)iz[(i/z)^{1/2}\coth(i/z)^{1/2} - 1]}, \tag{19}$$

where $z = D/(\omega R_0^2)$ and D is the gas thermal diffusivity. The quantity p_0 is the undisturbed pressure in the bubble and is given by $p_0 = P_0 + 2\sigma/R_0$, where P_0 denotes the equilibrium pressure in the liquid. The damping coefficient δ_t is the sum of three components: the viscous damping constant, the damping constant due to thermal effects and the acoustic radiation damping constant:

$$\delta_t = \frac{4\mu}{\rho_0 \omega R_0^2} + \frac{p_0}{\rho_0 R_0^2 \omega^2}\mathrm{Im}\,\Phi + \frac{\omega R_0}{c_0}, \tag{20}$$

where μ is the coefficient of molecular viscosity of seawater.

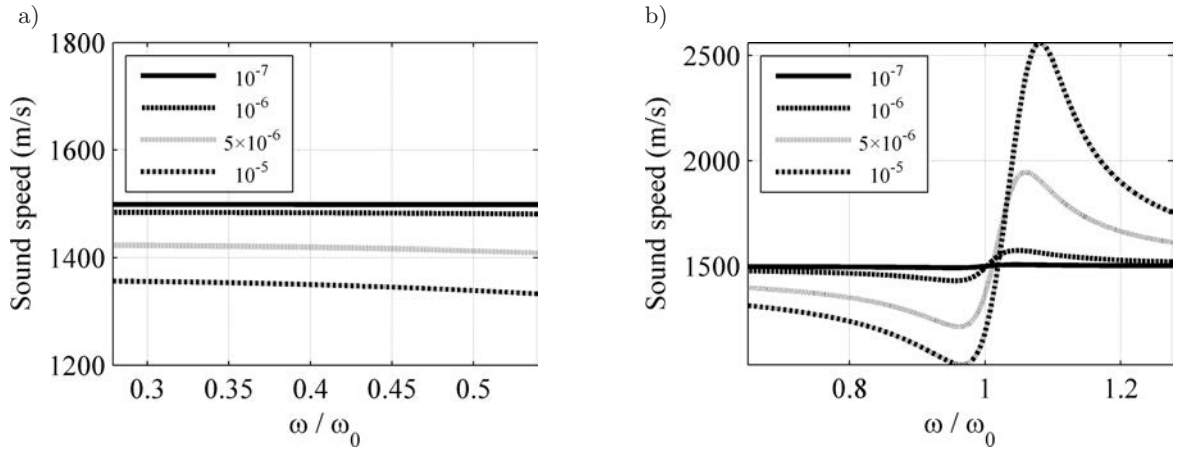

Fig. 2. The phase sound speed as function of signal frequency normalized by the bubble resonance frequency for different values of bubble radii and volume fractions: a) $R_0 = 40$ μm, b) $R_0 = 100$ μm.

We have analyzed signals which frequencies f are in the region from 20 kHz to 40 kHz. The results of the numerical investigations presented here are for two values of the bubble radius. In the first case, the bubble population is not resonant with the incident wave ($R_0 = 40$ μm) and in the second one this population is resonant with the incident wave ($R_0 = 100$ μm). Figure 2 depicts the phase sound speed as function of signal frequency normalized by the bubble resonance frequency. The curves show the results obtained for different values of bubble radius and volume fraction. For the frequency $f = 30$ kHz and radius $R_0 = 40$ μm, the resonance frequency equals $f_0 = 73.1$ kHz. Similarly, for $R_0 = 100$ μm we obtain $f_0 = 31.9$ kHz. We put here $c_0 = 1500$ m/s, $\rho_0 = 1000$ kg/m^3, $P_0 = 100$ kPa, $\sigma = 0.07$ N/m, $\mu = 0.001$ Ns/m^2 and $\gamma = 1.4$. The sound speed changes are large when the source frequency is not far from the resonance one. Near the resonance frequency of the bubbles, when the sounding frequency increases above or decreases below the resonance frequency of a single sized bubble population, the acoustic impedance in the layer becomes essentially different from that obtained in the case of a pure liquid. One of the results is an increase of the reflection coefficient.

4. Results of numerical investigations

The first step of our theoretical analysis was the study of influence of frequency and layer thickness on the transmitted and reflected waves. Figure 3 depicts the first and second harmonic amplitudes of transmitted waves normalized by the pressure $P_A = 40$ kPa calculated numerically assuming that a harmonic wave is propagated in the bubble layer. We put the sound speed $c_0 = 1500$ m/s and density $\rho_0 = 1000$ kg/m^3. The values of the speed c_L, which depend on the sound frequency were calculated using the Commander and Prosperreti model. The numerical calculations were made for different values of volume fraction assuming

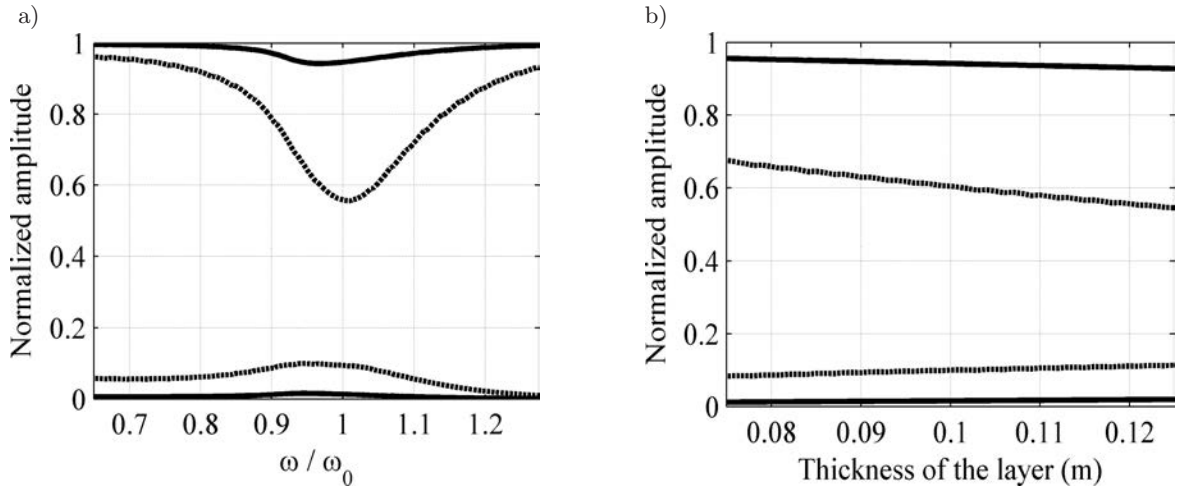

Fig. 3. The first and the second harmonic amplitudes of the transmitted waves normalized by the pressure P_A for volume fractions $\beta_0 = 10^{-7}$ (solid line) and $\beta_0 = 10^{-6}$ (dashed line): $P_A = 40$ kPa, $R_0 = 100$ μm; a) $L = 0.1$ m, b) $f = 30$ kHz.

that the bubble radius is $R_0 = 100$ μm. The pressure amplitudes of the transmitted wave as function of signal frequency normalized by the bubble resonance frequency for the layers of thickness $L = 0.1$ m are presented in Fig. 3a. The result obtained for the same pressure amplitudes as a function of layer thickness for the incident wave frequency $f = 30$ kHz is given in Fig. 3b. The pressure amplitudes of the reflected wave obtained for the volume fraction $\beta_0 = 10^{-7}$ are presented in Fig. 4. The values of the remaining physical and numerical parameters are the same as used earlier.

The values of the volume fraction have a great influence on the pressure distribution inside the layer. For this reason, the effect of this parameter on the nonlinear generation was more thoroughly examined. Figure 5 shows normalized amplitudes of the first and second harmonics in the transmitted wave as function of volume fraction calculated for different values of the bubble radius. Figure 5a shows the result obtained for $R_0 = 100$ μm. In this case the amplitude of the first harmonic decreases very quickly, while the amplitude of the second one increases for small values of the volume fraction and then it stabilizes. An example of the results of calculations obtained for bubble radius not resonant presents Fig. 5b. Figure 6 presents the first and the second harmonic amplitudes of the transmitted and reflected waves normalized by pressure P_A as functions of volume fraction for $R_0 = 40$ μm, $L = 0.1$ m, $f = 30$ kHz and $P_A = 20$ kPa.

The distributions normalized by pressure P_A of the first and the second harmonic amplitudes of the transmitted and reflected waves at frequency $f = 30$ kHz, amplitude $P_A = 20$ kPa and bubble radius $R_0 = 40$ μm for different layer thicknesses and different values of volume fraction are represented in Fig. 7. Figure 8 shows similar results obtained for $R_0 = 100$ μm.

The last step of our theoretical investigations was devoted to a theoretical analysis of the relationship

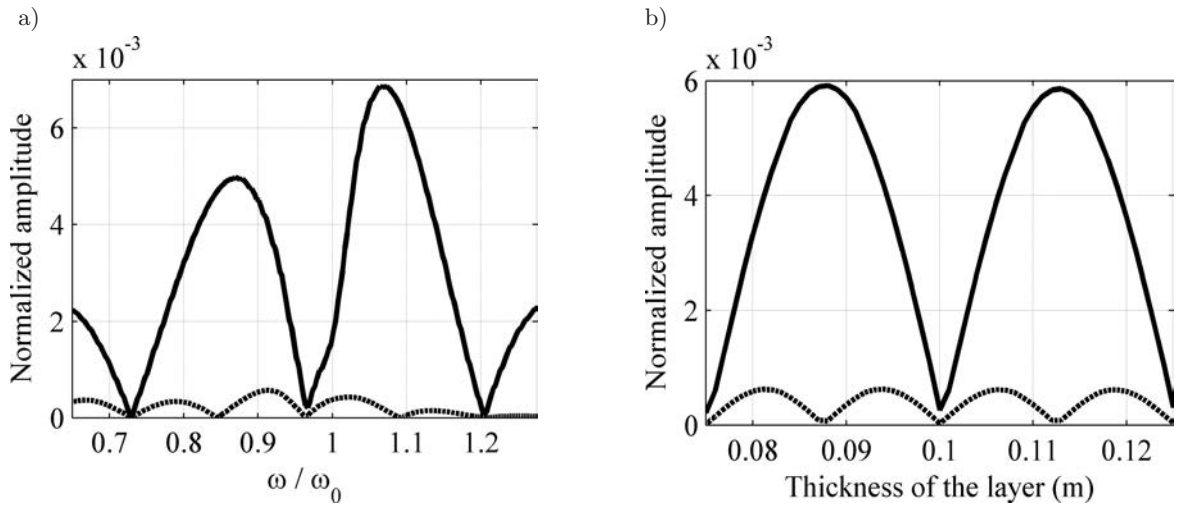

Fig. 4. The first (solid line) and second (dashed line) harmonic amplitudes of the reflected wave normalized by the pressure $P_A = 40$ kPa, $R_0 = 100$ μm, $\beta_0 = 10^{-7}$: a) $L = 0.1$ m, b) $f = 30$ kHz.

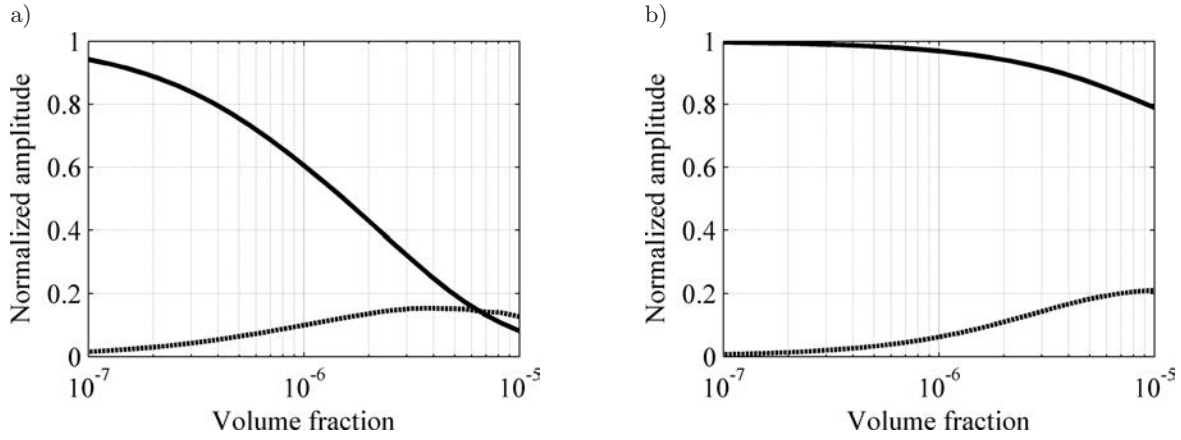

Fig. 5. The first harmonic amplitude (solid line) and the second one (dashed line) of the transmitted wave normalized by pressure P_A as functions of volume fraction for $f = 30$ kHz, $P_A = 40$ kPa and $L = 0.1$ m: a) $R_0 = 100$ μm, b) $R_0 = 40$ μm.

between the first and second harmonic amplitudes of the transmitted and reflected waves, respectively. Figure 9a presents the second harmonic amplitudes of the transmitted wave normalized by their first harmonic amplitudes as functions of volume fraction obtained for $f = 30$ kHz, different values of the incident wave amplitude and fixed values of the bubble radius. Similar results obtained for the reflected wave depicts Fig. 9b. Figure 10 shows an example of distribution of the second harmonic amplitude of the transmitted wave normalized by the first harmonic amplitude. The calculations were made for different layer thicknesses and different values of volume fractions at $f = 30$ kHz, $P_A = 20$ kPa and $R_0 = 40$ μm.

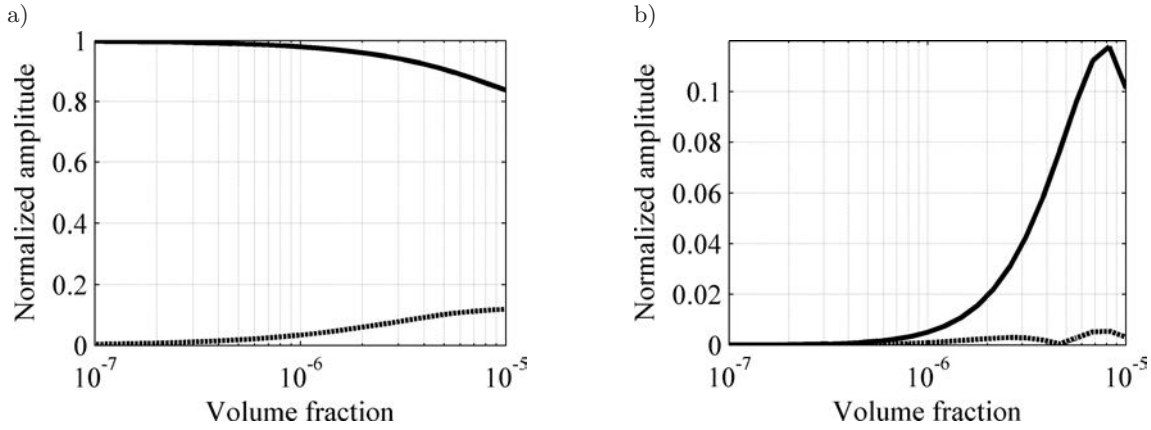

Fig. 6. The first harmonic amplitude (solid line) and the second one (dashed line) of the transmitted wave (a) and the reflected one (b) normalized by pressure P_A as functions of volume fraction; $f = 30$ kHz, $P_A = 20$ kPa, $L = 0.1$ m, $R_0 = 40$ μm.

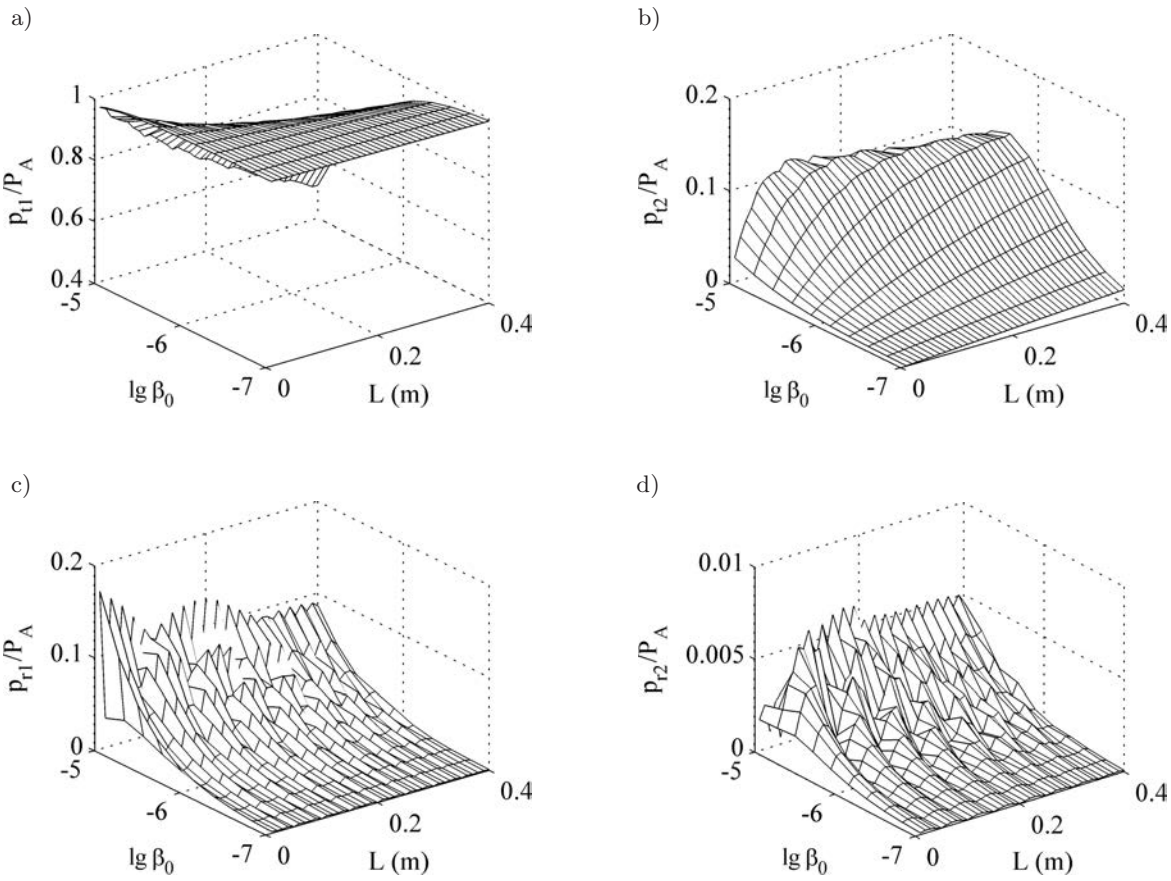

Fig. 7. The space distribution of the first and the second harmonic amplitude of the transmitted and reflected waves normalized by pressure P_A: $f = 30$ kHz, $P_A = 20$ kPa, $R_0 = 40$ μm.

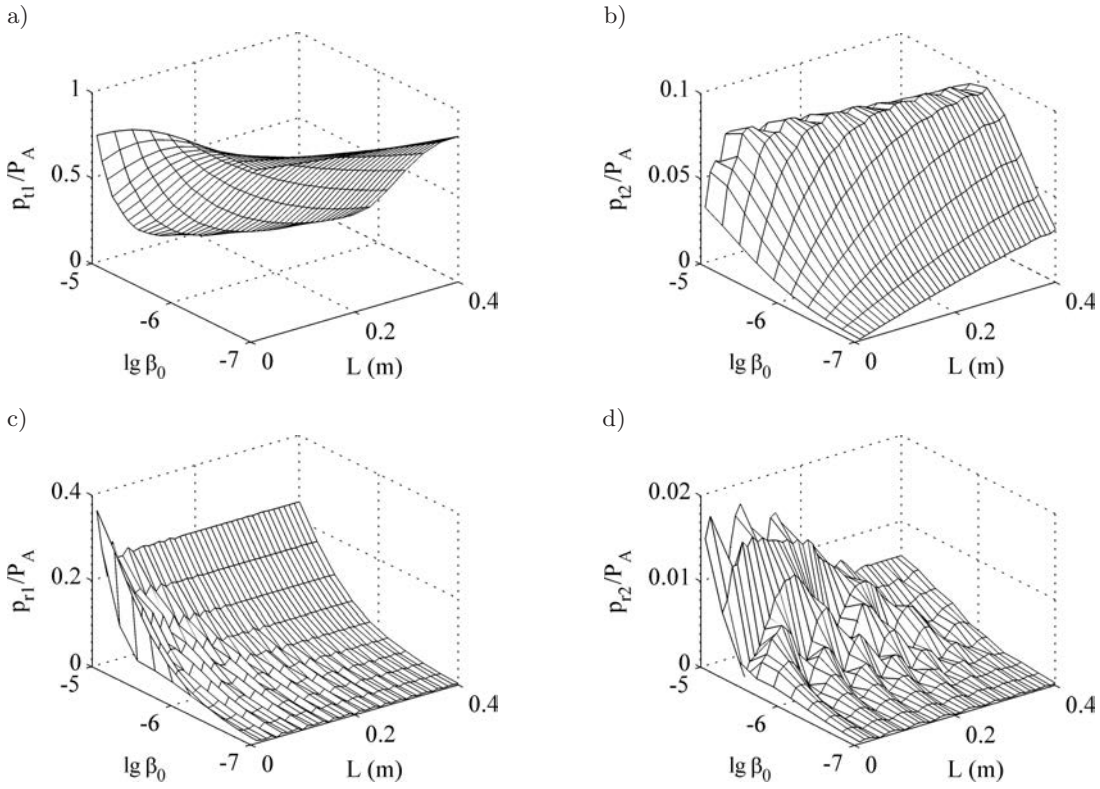

Fig. 8. The space distribution of the first and the second harmonic amplitudes of the transmitted and reflected waves normalized by pressure P_A; $f = 30$ kHz, $P_A = 20$ kPa, $R_0 = 100$ μm.

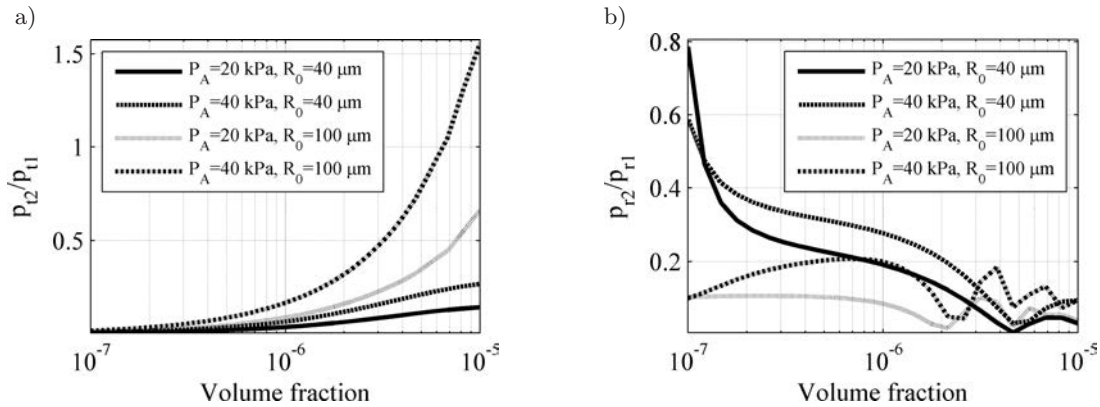

Fig. 9. The second harmonic amplitude of the transmitted (a) and reflected (b) waves normalized by their first harmonic amplitudes as functions of volume fraction; $f = 30$ kHz, $L = 0.1$ m.

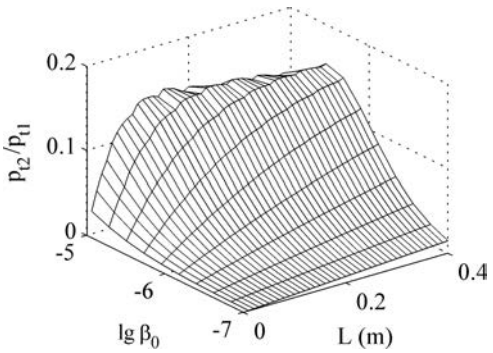

Fig. 10. The space distribution of the second harmonic amplitude of the transmitted wave normalized by the first harmonic amplitude; $f = 30$ kHz, $P_A = 20$ kPa, $R_0 = 40$ μm.

5. Conclusions

The problem of the efficiency of the higher harmonic generation in a bubbly liquid layer was considered and its mathematical model was constructed on the basis of two presented differential equations. Some results of the numerical investigations were discussed. The linear non-dissipative wave equation was solved numerically by employing the finite-difference method. The Rayleigh–Plesset equation describing the bubble oscillation was solved using the classical fourth order Runge–Kutta method. The changes of the transmitted and reflected waves were examined. Numerical cal-

culations were carried out using a computer program specially designed for this problem by the author.

The purpose of the paper was to conduct numerical investigations of the nonlinear generation by a bubble layer. Many different environmental and sounding signal parameters have an influence on the nonlinear waves propagation over the bubble layer. The influences of fixed environmental and sounding signal parameters on the second harmonic amplitudes of the transmitted and reflected waves were analyzed. First of all, the numerical calculations were made for different values of the layer thickness and volume fractions, as well as for different values of frequency and pressure amplitudes of the generated signals. A detailed analysis carried out for different sizes of bubbles shows how significant influence on the nonlinear generation efficiency has the gas void fraction. For example, when the frequency of sounding signal is fixed, we observe a larger attenuation of the first harmonic amplitude of the transmitted wave in case of resonant bubbles, than in that of bubbles with different radii. Near the resonance frequency of the bubbles, the acoustic impedance in the layer becomes significantly different from that obtained in case of a pure liquid and as a consequence the reflection coefficient increases. The results of numerical investigations show also that when the bubble population is not resonant, it is possible to find values of the layer thickness or the volume fraction for which the ratios of the second harmonic amplitudes of the transmitted wave to their first harmonic amplitudes are the greatest and, in consequence, the nonlinear generation efficiency is the best. It is much more difficult to find such values of these parameters when the bubbles frequency is resonant.

All the results presented in this paper were obtained assuming that the single bubble layer is surrounded by media with contrasting physical properties. Although this paper deals with the harmonic wave propagation only, it is not difficult to extend this model to the case of more than one layer having different features. It is also possible to develop computer programs for biharmonic waves as well as for continuous signals and impulse signals with different envelopes. This model can be useful in studying the wave propagation in a bubbly environment, for example, it can be employed in the simulation of the efficiency of parametric sonars operating in different forms of the nonlinear layer.

Acknowledgment

This article is an extended version of the paper "Numerical testing of nonlinear generation efficiency in a bubble layer" presented at the 58th Open Seminar on Acoustics, OSA 2011, September 13–16, 2011, Jurata, Poland.

References

1. Baranowska A. (2011), *Numerical modeling of the nonlinear wave propagation in a bubble layer*, Hydroacoustics, **14**, 9–16.
2. Commander W., Prosperetti A. (1989), *Linear pressure waves in bubbly liquids: Comparison between theory and experiments*, Journal of the Acoustical Society of America, **85**, 732–746.
3. Druzhinin O.A., Ostrovsky L.A., Prosperetti A. (1996), *Low-frequency acoustic wave generation in a resonant bubble layer*, Journal of the Acoustical Society of America, **100**, 6, 3570–3580.
4. Hamilton M.F., Blackstock D.T. [Eds.] (1998), *Nonlinear Acoustics*, Academy Press, San Diego.
5. Karpov S., Prosperetti A., Ostrovsky L. (2003), *Nonlinear wave interactions in bubble layers*, Journal of the Acoustical Society of America, **113**, 3, 1304–1316.
6. Leighton T.G. (2008), *The Rayleigh-Plesset equation in terms of volume with explicit shear losses*, Ultrasonics, **48**, 85–90.
7. Perelomova A., Wojda P. (2010), *Studies of nonlinear sound dynamics in fluids based on the caloric equation of state*, Archives of Acoustics, **35**, 4, 619–633.
8. Vanhille C., Campos–Pozuelo C. (2008), *Nonlinear ultrasonic propagation in bubbly liquids: a numerical model*, Ultrasounds in Medicine and Biology, **34**, 5, 792–808.
9. Ye Z., Ding L. (1995), *Acoustic dispersion and attenuation relations in bubbly mixture*, Journal of the Acoustical Society of America, **98**, 1629–1636.